

# **In-Situ Studies of the Growth of Amorphous and Microcrystalline Silicon Using Real-Time Spectroscopic Ellipsometry**

D. Levi, B. Nelson, and J. Perkins

*Presented at the National Center for Photovoltaics and Solar Program Review Meeting  
Denver, Colorado  
March 24-26, 2003*



**NREL**

**National Renewable Energy Laboratory**

1617 Cole Boulevard  
Golden, Colorado 80401-3393

NREL is a U.S. Department of Energy Laboratory  
Operated by Midwest Research Institute • Battelle • Bechtel

Contract No. DE-AC36-99-GO10337

## NOTICE

The submitted manuscript has been offered by an employee of the Midwest Research Institute (MRI), a contractor of the US Government under Contract No. DE-AC36-99GO10337. Accordingly, the US Government and MRI retain a nonexclusive royalty-free license to publish or reproduce the published form of this contribution, or allow others to do so, for US Government purposes.

This report was prepared as an account of work sponsored by an agency of the United States government. Neither the United States government nor any agency thereof, nor any of their employees, makes any warranty, express or implied, or assumes any legal liability or responsibility for the accuracy, completeness, or usefulness of any information, apparatus, product, or process disclosed, or represents that its use would not infringe privately owned rights. Reference herein to any specific commercial product, process, or service by trade name, trademark, manufacturer, or otherwise does not necessarily constitute or imply its endorsement, recommendation, or favoring by the United States government or any agency thereof. The views and opinions of authors expressed herein do not necessarily state or reflect those of the United States government or any agency thereof.

Available electronically at <http://www.osti.gov/bridge>

Available for a processing fee to U.S. Department of Energy  
and its contractors, in paper, from:

U.S. Department of Energy  
Office of Scientific and Technical Information  
P.O. Box 62  
Oak Ridge, TN 37831-0062  
phone: 865.576.8401  
fax: 865.576.5728  
email: [reports@adonis.osti.gov](mailto:reports@adonis.osti.gov)

Available for sale to the public, in paper, from:

U.S. Department of Commerce  
National Technical Information Service  
5285 Port Royal Road  
Springfield, VA 22161  
phone: 800.553.6847  
fax: 703.605.6900  
email: [orders@ntis.fedworld.gov](mailto:orders@ntis.fedworld.gov)  
online ordering: <http://www.ntis.gov/ordering.htm>



# In-Situ Studies of the Growth of Amorphous and Microcrystalline Silicon Using Real-Time Spectroscopic Ellipsometry

D. Levi, B. Nelson, and J. Perkins  
National Renewable Energy Laboratory  
1617 Cole Blvd., Golden CO, 80401 USA

## ABSTRACT

Real-time, in-situ characterization of hot-wire chemical vapor deposition (HWCVD) growth of hydrogenated silicon (Si:H) thin films offers unique insight into the properties of the materials and mechanisms of their growth. We have used in-situ spectroscopic ellipsometry to characterize Si:H crystallinity as a function of film thickness and deposition conditions. We find that the transition from amorphous to microcrystalline growth is a strong function of film thickness and hydrogen dilution, and a weak function of substrate temperature. We have expressed this information in terms of a color-coded phase-space map of the amorphous to microcrystalline transition in HWCVD growth on crystalline Si substrates.

## 1. Introduction

In-situ real-time spectroscopic ellipsometry (RTSE) is a valuable new technique for characterization of material properties in real time during film growth. We have applied this technique to study the properties of amorphous (a-Si:H) and microcrystalline ( $\mu$ c-Si:H) hydrogenated silicon grown using HWCVD. We report here on the results of this work over the past 15 months.

RTSE measures the optical properties of the growing film as rapidly as 5 times per second. The primary parameters characterized are the film thickness, dielectric function, and surface roughness. The dielectric function provides a sensitive measure of the degree of crystallinity of the film. Film thickness vs. time provides an accurate measure of the growth rate. Changes in the surface roughness provide indications of transitions from one mode of growth to another [1].

## 2. Experimental Details

HWCVD deposition of Si:H films was performed using a single 0.5-mm-diameter W filament operated at a 60-Hz ac filament current of 16 amps ( $\sim 2200^\circ\text{C}$ ). The filament is wrapped in a 4-mm-diameter helix and mounted 4 cm from the substrates. The silane flow was fixed to 6 sccm with a silane partial pressure of  $\sim 3$  mTorr. The two main deposition parameters varied in this study were the substrate heater temperature ( $T_H$ ), at either  $250^\circ$  or  $500^\circ\text{C}$ , and hydrogen dilution ratio ( $R=\text{SiH}_4/\text{SiH}_4+\text{H}_2$ ) from 0 to 14. All films were grown to a thickness of about 1  $\mu\text{m}$ . These experiments were carried out in the same chamber described in detail in [2] and under similar conditions to those in [3].

RTSE measurements were performed using a J.A. Woollam, Inc., M2000 visible and near-infrared rotating compensator ellipsometer and Woollam software for

instrument control and data acquisition and analysis. The ellipsometer uses array detectors to collect spectra from 250 to 1700 nm, with an acquisition time as short as 200 ms. For this study, spectra were collected from 255 to 1240 nm, with an integration time of 200 to 500 ms during the nucleation phase of growth and 1 to 5 seconds during the later stages of growth, dependent on film deposition rates. The angle of incidence was fixed at  $70^\circ$ .

The Raman scattering measurements were performed in a 180-degree backscattering configuration with a doubled Nd:YAG laser operating at 532 nm and a single-grating Spex 270M spectrometer with a LN<sub>2</sub>-cooled CCD array detector. The incident laser power was 30 mW, and a holographic notch filter was used to suppress the laser line. Penetration depth was about 96 nm for  $\mu\text{c-Si:H}$  and 64 nm for a-Si:H.

## 3. Analysis of RTSE Results

Ellipsometry data are expressed in terms of the amplitude ratio  $\Psi$  and the phase angle  $\Delta$ . These data are translated into physical information about the sample through model-based analysis [4]. The Fresnel equations are used to calculate  $\Psi_{\text{th}}$  and  $\Delta_{\text{th}}$  from a theoretical model of the growing film. These values are then compared with  $\Psi_{\text{exp}}$  and  $\Delta_{\text{exp}}$  to calculate a mean-squared error (MSE). Parameters in the model are adjusted using Levenburg-Marquardt optimization to minimize the MSE.

Models used in this study include several layers; the crystalline Si substrate, the native oxide on top of the substrate, the Si:H, and a surface roughness layer. Primary experimental variables that are derived through analysis are the thickness and optical properties of the Si:H and the surface roughness. The optical properties are expressed in terms of the dielectric function or dielectric spectrum, which is closely related to the electronic properties of the material.

RTSE data consist of a time series of ellipsometric spectra. The model is fit sequentially to each spectrum, with the final fit parameters of one time-step providing the starting point for fitting the next time-step. The entire time series of data is fit iteratively. An initial guess for the dielectric function of the Si:H is fit to the data to provide an initial sequence of layer thickness values  $d_i(t)$ . A subset of these thickness values is then used to calculate an optimized dielectric function that minimizes the total MSE over this subset. This dielectric function is then applied to the entire time sequence to generate an improved set of thickness values. These values are, in turn, used to generate a third-generation dielectric function. This process is repeated until it is no longer possible to reduce the total MSE. Additional layers may be included in the model as necessary to minimize the error. The thickness at each time-step for each layer in the model is determined through a sequential fit to

the time-sequence data, with the only constraint on  $d_i(t)$  being minimization of the MSE.

RTSE data were analyzed in two stages. The early-time nucleation phase was modeled using a two-layer model, consisting of a bulk film with thickness  $d_b$  and a surface-roughness layer with thickness  $d_s$ , both on top of a crystalline silicon substrate with a  $\sim 15$ -Å-thick native oxide layer. Most of the growth conditions required a third layer to represent a secondary phase of Si:H that started growing shortly after the nucleation phase had coalesced. The surface roughness layer was modeled using a Bruggeman effective medium approximation (EMA) of 50% void and 50% of the underlying material. The dielectric functions of the nucleation and post-nucleation layers were determined using the iterative optimization method to minimize the MSE within a selected region of growth time. Amorphous Si:H was modeled using a Cody-Lorentz oscillator formalism, whereas microcrystalline Si:H was modeled using a two-oscillator Tauc-Lorentz formalism [5].

In most of the films studied, the optical properties of the film evolved during deposition. Multilayer models do not work well to analyze the data as the film grows because of grading in the optical properties. To analyze the data after the initial nucleation phase, we have used a virtual interface (VI) model. The VI model cannot be applied during nucleation because it assumes a slowly varying surface roughness. The VI model fits the data using a 3-layer model consisting of 1) a surface roughness layer on top of 2) a growing film of thickness  $5rt_0$ , where  $r$  is the growth rate and  $t_0$  is the data acquisition interval, and 3) a pseudo-substrate with a pseudo-dielectric function  $\langle \epsilon \rangle$  calculated by directly inverting the  $\Psi$  and  $\Delta$  data at time  $t_{n-5}$ . The growing film of thickness  $5rt_0$  is modeled as a 2-component Bruggeman EMA composed of a mixture of materials determined from the post-nucleation layer and the final material deposited at the end of the deposition. The growth rate  $r$  is held constant, whereas the EMA percentage and surface roughness thickness are fit using regression analysis. In general, for each film, three distinct dielectric functions are determined corresponding to the nucleation layer, mid-layer, and final layer. In the more homogeneous films, some or all of these layers may be the same.

#### 4. Analysis of Crystallinity

The degree of crystallinity of the films in this study was analyzed using in-situ RTSE and ex-situ Raman scattering. Raman scattering provides a semi-quantitative measure of crystallinity through the relative amplitudes of the amorphous and microcrystalline Raman peaks. Ellipsometry provides information on the degree of crystallinity from the dielectric function derived through analysis of the RTSE data. Whereas Raman scattering provides an average weighted by the intensity of the laser vs. depth, RTSE is able to provide a qualitative map of the crystallinity vs. depth in the film.

Figure 1 presents Raman scattering spectra for the  $T_s=250^\circ\text{C}$  films. The broad peak at  $\sim 460\text{ cm}^{-1}$  is correlated with amorphous, whereas the sharp peak at  $\sim 520\text{ cm}^{-1}$  is correlated with microcrystalline silicon [6]. Penetration

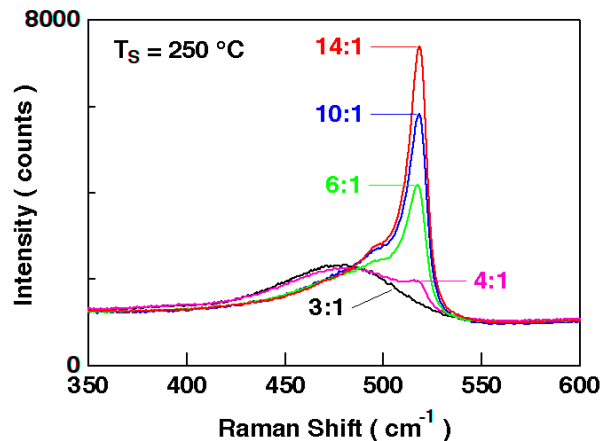


Figure 1. Raman scattering spectra for samples grown at  $T_H=250^\circ\text{C}$ .

depths calculated at the 532-nm laser wavelength are 96 nm for microcrystalline and 64 nm for amorphous silicon. Because the degree of crystallinity varies with depth in the film, it is difficult to calculate an accurate ratio of amorphous to microcrystalline material based on the Raman scattering peak heights. The Raman data do provide a qualitative measure of the relative degree of crystallinity within the top  $0.1\ \mu\text{m}$  of these  $1.0\text{-}\mu\text{m}$ -thick samples. In addition, the Raman intensity scales with the degree of crystallinity, with small-grained  $\mu\text{c-Si:H}$  having a lower Raman intensity than large-grained  $\mu\text{c-Si:H}$ , and crystalline Si having a much higher intensity than any of the  $\mu\text{c-Si:H}$  samples measured in this study. We attribute this to final-state lifetime effects on the Raman scattering cross-section. Thus, the amplitude of the  $520\text{ cm}^{-1}$  peak in the Raman spectrum is an indication of the degree of crystallinity of the upper layer of the  $\mu\text{c-Si:H}$  films.

It is clear in Fig. 1 that the  $R=0$  and  $R=3$  films are purely a-Si:H near the surface, whereas the  $R=4$  film has a slight degree of crystallinity. The  $R=6$ , 10, and 14 films are all predominantly  $\mu\text{c-Si:H}$  near the surface, with varying peak heights. This likely correlates with grain size in these  $\mu\text{c-Si:H}$  films.

Figure 2 illustrates how the real ( $\epsilon_1$ ) and imaginary ( $\epsilon_2$ ) parts of the dielectric function evolve with the degree of crystallinity of the film. Figure 2 (a) shows the real part of the dielectric function  $\epsilon_1$ , and Fig. 2 (b) shows the imaginary part of the dielectric function  $\epsilon_2$ .  $\epsilon_1$  relates to the index of refraction  $n$ , whereas  $\epsilon_2$  relates to the extinction coefficient  $k$ . The curves in yellow are for pure a-Si:H, the red curves show  $\epsilon_1$  and  $\epsilon_2$  for mixed a-Si:H and  $\mu\text{c-Si:H}$ , and the black curves are for pure  $\mu\text{c-Si:H}$ . As the film evolves from a-Si:H to  $\mu\text{c-Si:H}$ , both the amplitude and the peak energy of  $\epsilon_1$  and  $\epsilon_2$  increase. The amplitude of  $\epsilon_1$  and  $\epsilon_2$  are also influenced by the presence of voids in the material. Because of this ambiguity in tracking the crystallinity using the amplitude of the dielectric function, we have focused on the

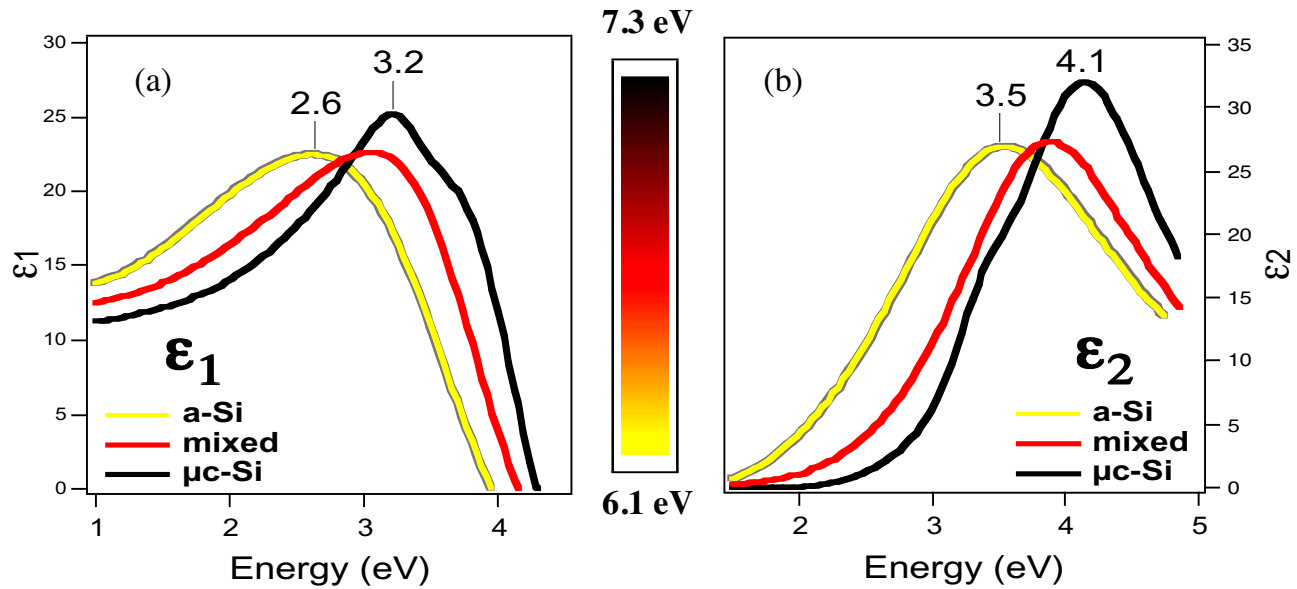


Figure 2. Real (a) and imaginary (b) parts of the dielectric function for amorphous (yellow), mixed amorphous and microcrystalline (red), and purely microcrystalline (black) Si:H. The color scale in the middle illustrates how the sum of the  $\epsilon_1$  and  $\epsilon_2$  peak energies are converted into a continuous amorphous to microcrystalline color scale.

peak energies for  $\epsilon_1$  and  $\epsilon_2$ . By summing the peak energy of the real and imaginary parts of the dielectric function, we have a numerical scale that ranges from 6.1 eV to 7.3 eV, corresponding to pure a-Si:H at 6.1 eV and pure  $\mu$ c-Si:H at 7.3 eV. This scale is expressed in terms of color in the color bar at the center of Fig. 2, with yellow corresponding to the lowest energy sum and black corresponding to the highest energy sum.

Figure 3 is a representation of the degree of crystallinity versus depth based on the dielectric functions measured in-situ using RTSE. Note that films grown at  $T_s=250^\circ\text{C}$  have a higher hydrogen content, which shifts the peak energies of the dielectric function higher. Thus, even completely amorphous films at this temperature will have a slight orange shading, instead of being completely yellow.

As described in the section on analysis, most films required three distinct dielectric functions for analysis of the in-situ RTSE data. This consisted of one function for the nucleation phase, one for the intermediate phase, and one for the end phase. Nucleation was described as a single or double layer, with the nucleation layer thickness allowed to vary as needed to fit the RTSE data. The remainder of the film was modeled as an EMA mixture of the intermediate and final dielectric functions. Thus, the EMA % value provides a continuous scale between the intermediate and final endpoints. Although this is only a semiquantitative approach to describing the crystallinity versus thickness, we believe that the results accurately describe how the relative degree of crystallinity evolves with substrate temperature, hydrogen dilution, and film thickness.

Figure 3 (a) presents the evolution of crystallinity with thickness and hydrogen dilution for  $T_s=250^\circ\text{C}$ . The numbers across the top give the ratio of the amplitude of

the  $520\text{ cm}^{-1}$  peak in the Raman spectrum to the highest intensity  $520\text{ cm}^{-1}$  peak measured in this study. This number is roughly interpreted as the relative degree of crystallinity within the uppermost  $1000\text{ \AA}$  of the film. The homogeneous orange color for the R=0 and R=3 films in Fig. 3 (a) show that the R=0 and R=3 films are completely amorphous. This is confirmed by the Raman results. The R=4 film appears to be completely amorphous in the RTSE data, yet Raman indicates a small component of microcrystalline material at the surface. The R=6 film nucleates as a-Si:H, and grows primarily as  $\mu$ c-Si:H. The R=10 film nucleates as a material that appears to be midway between a-Si:H and  $\mu$ c-Si:H, whereas the bulk of its growth is microcrystalline. Finally, the R=14 film is  $\mu$ c-Si:H at nucleation and throughout its growth.

Trends are very similar for the  $T_s=500^\circ\text{C}$  films shown in Fig. 3 (b). The R=0 and R=3 films are completely amorphous. Although the R=4 film nucleates as a-Si:H, it has a significantly greater  $\mu$ c-Si:H component than the  $T_s=250^\circ\text{C}$  R=4 film. This is confirmed by the Raman results. The R=6 film nucleates as a-Si:H and becomes increasingly crystalline as thickness increases. The R=10 and R=14 films show somewhat distinct behavior. The R=10 film nucleates as mixed phase, transitions to a more-crystalline mixed phase, and then becomes less crystalline as it increases in thickness. The R=14 film nucleates as  $\mu$ c-Si:H and appears to make a transition to mixed a-Si:H and  $\mu$ c-Si:H after the nucleation phase. After that, the film becomes increasingly crystalline as it grows. These two films present a somewhat puzzling result. We believe it may be related to the template effect of the crystalline substrate. In the nucleation phase, the growth may be epitaxial, producing highly crystalline material. Once the film reaches a critical thickness, the epitaxial registry is lost and the film makes a transition to mixed amorphous-

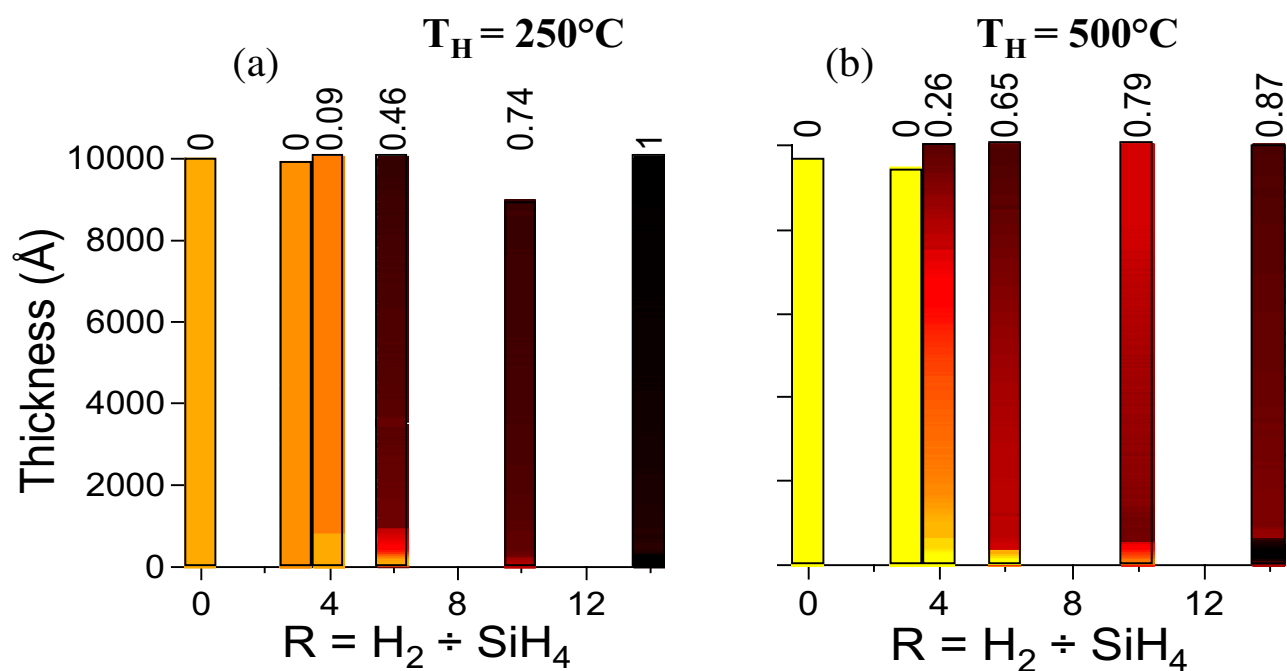


Figure 3. Color scale phase map of crystallinity vs. dilution and thickness for HWCVD Si:H films grown at (a) T<sub>H</sub>=250°C, and (b) T<sub>H</sub>=500°C.

microcrystalline growth. The results are still somewhat puzzling because of the different evolution of the two films after nucleation. We plan to reproduce these conditions to clarify this issue in the future.

#### 4. Discussion and Conclusions

Based on Fig. 3, we can draw some conclusions about the transition from a-Si:H to  $\mu$ c-Si:H growth for HWCVD deposition of Si:H on crystalline silicon substrates. For both deposition temperatures studied, it is clear that the transition is a gradual one, both in dilution and film thickness. For T<sub>H</sub>=250°C, mixed-phase growth emerges near 1000-Å thickness at R=6. This transition occurs earlier for the T<sub>H</sub>=500°C conditions. At the higher temperature, mixed-phase growth is first seen near 2000 – 4000-Å thickness at R=4. An important point to note is that the transition is a function of both dilution and film thickness. If we were only to consider the Raman scattering results, we would conclude that the transition occurs at R=4 for both growth temperatures; in this case, we can see that the thickness of the film has a dramatic effect on the degree of crystallinity.

A second important point is that there is a broad range of conditions where the growth is mixed-phase. The films are not predominantly  $\mu$ c-Si:H until R=14 or beyond. In the transition region, the degree of crystallinity is a strong function of film thickness. This information should be valuable input for thin-film Si:H device growth. Our future plans include studies of HWCVD growth on substrates designed to mimic those used for device growth.

#### REFERENCES

1. R.W. Collins, J. Koh, H. Fujiwara, P.I. Rovira, A.S. Ferlauto, J.A. Zapien, C.R. Wronski, and R. Messier, *Appl. Surf. Sci.*, **154-155**, 217-228 (2000).
2. B.P. Nelson, et al. MRS Conference Proceedings, San Francisco, CA, April, 2002, A17.3, 159-164.
3. D.H. Levi, et al. MRS Conference Proceedings, San Francisco, CA, April, 2002, A25.2, 153-158.
4. D.H. Levi, B.P. Nelson, J.D. Perkins, and H.R. Moutinho, Proceedings of the 29<sup>th</sup> IEEE Photovoltaic Specialists Conference, New Orleans, LA, May 2002, in press.
5. A.S. Ferlauto, G.M. Ferreira, C. Chen, P.I. Rovira, C.R. Wronski, R.W. Collins, X. Deng, and G. Ganguly, "Optical metrology for the next generation of a-Si:H-based thin film photovoltaics," *Photovoltaics for the 21<sup>st</sup> Century II*, ed R.D. McConnell and V.K. Kapur (The Electrochemical Society, 2001) pp.199-228
6. G. Yue, J. D. Lorentzen, J. Lin, Q. Wang and D. Han, *APL*. **75**, 492 (1999).

REPORT DOCUMENTATION PAGE			Form Approved OMB NO. 0704-0188	
Public reporting burden for this collection of information is estimated to average 1 hour per response, including the time for reviewing instructions, searching existing data sources, gathering and maintaining the data needed, and completing and reviewing the collection of information. Send comments regarding this burden estimate or any other aspect of this collection of information, including suggestions for reducing this burden, to Washington Headquarters Services, Directorate for Information Operations and Reports, 1215 Jefferson Davis Highway, Suite 1204, Arlington, VA 22202-4302, and to the Office of Management and Budget, Paperwork Reduction Project (0704-0188), Washington, DC 20503.				
1. AGENCY USE ONLY (Leave blank)	2. REPORT DATE May 2003	3. REPORT TYPE AND DATES COVERED Conference Paper		
4. TITLE AND SUBTITLE In-Situ Studies of the Growth of Amorphous and Microcrystalline Silicon Using Real-Time Spectroscopic Ellipsometry			5. FUNDING NUMBERS PVP3.3101	
6. AUTHOR(S) D. Levi, B. Nelson, J. Perkins				
7. PERFORMING ORGANIZATION NAME(S) AND ADDRESS(ES) National Renewable Energy Laboratory 1617 Cole Blvd. Golden, CO 80401-3393			8. PERFORMING ORGANIZATION REPORT NUMBER NREL/CP-520-33571	
9. SPONSORING/MONITORING AGENCY NAME(S) AND ADDRESS(ES)			10. SPONSORING/MONITORING AGENCY REPORT NUMBER	
11. SUPPLEMENTARY NOTES				
12a. DISTRIBUTION/AVAILABILITY STATEMENT National Technical Information Service U.S. Department of Commerce 5285 Port Royal Road Springfield, VA 22161			12b. DISTRIBUTION CODE	
13. ABSTRACT ( <i>Maximum 200 words</i> ) Real-time, in-situ characterization of hot-wire chemical vapor deposition (HWCVD) growth of hydrogenated silicon (Si:H) thin films offers unique insight into the properties of the materials and mechanisms of their growth. We have used in-situ spectroscopic ellipsometry to characterize Si:H crystallinity as a function of film thickness and deposition conditions. We find that the transition from amorphous to microcrystalline growth is a strong function of film thickness and hydrogen dilution, and a weak function of substrate temperature. We have expressed this information in terms of a color-coded phase-space map of the amorphous to microcrystalline transition in HWCVD growth on crystalline Si substrates.				
14. SUBJECT TERMS characterization; real-time spectroscopic ellipsometry; hot-wire chemical vapor deposition; hydrogenated silicon; crystallinity			15. NUMBER OF PAGES	
			16. PRICE CODE	
17. SECURITY CLASSIFICATION OF REPORT Unclassified	18. SECURITY CLASSIFICATION OF THIS PAGE Unclassified	19. SECURITY CLASSIFICATION OF ABSTRACT Unclassified	20. LIMITATION OF ABSTRACT UL	